International Journal of Information, Control and Computer Sciences
ISSN: 2517-9942
Vol:9, No:6, 2015

Implicit Force Control of a Position Controlled Robot – A Comparison with Explicit Algorithms

Alexander Winkler, Jozef Suchý

Abstract—This paper investigates simple implicit force control algorithms realizable with industrial robots. A lot of approaches already published are difficult to implement in commercial robot controllers, because the access to the robot joint torques is necessary or the complete dynamic model of the manipulator is used. In the past we already deal with explicit force control of a position controlled robot. Well known schemes of implicit force control are stiffness control, damping control and impedance control. Using such algorithms the contact force cannot be set directly. It is further the result of controller impedance, environment impedance and the commanded robot motion/position. The relationships of these properties are worked out in this paper in detail for the chosen implicit approaches. They have been adapted to be implementable on a position controlled robot. The behaviors of stiffness control and damping control are verified by practical experiments. For this purpose a suitable test bed was configured. Using the full mechanical impedance within the controller structure will not be practical in the case when the robot is in physical contact with the environment. This fact will be verified by simulation.

Keywords—Damping control, impedance control, robot force control, stability, stiffness control.

I. Introduction

IN some fields of robot applications it is suitable to use force control instead of position control, e.g. when the robot is in physical contact with the environment or for some kinds of human-robot interaction. In the last decades the research field of robot force control has been investigated in depth and a lot of interesting concepts have been presented. An overview of different force control algorithms can be found e.g. in [1], [2] and [3]. One could think that the research field of force/torque control is completed, however, most of the industrial robots work only position controlled. It can be seen that force control only slowly finds its way from robotic laboratories into industry. For the purpose of accelerating this trend we think that force control algorithms should be as simple as possible to be realizable with commercial robot controllers. Additional attention has to be paid to the fact that we often have only access to the desired end-effector position, because access to joint torques or motor currents is not enabled by the manufacturer. So the force control loop is closed around the position control loop which leads to the so called position based force control approach [4], [5].

Generally, force control algorithms can be classified into explicit and implicit force control [1]. In explicit force control the contact forces and torques between end-effector and the environment (Env.) are compared with the desired values of the contact forces/torques. From their difference a convenient motion of the manipulator arm is generated with the aim to reach the desired force. A simplified signal flow diagram of explicit force control can be seen in Fig. 1. The current contact forces/torques measured by force/torque sensor (FTS) are represented by vector $\mathbf{F}$ .The vectors $\mathbf{F_d}$, $\mathbf{X}$ and $\mathbf{U}$ include the desired contact forces/torques, the current end-effector position/orientation and the generalized controller outputs, respectively. In the case that the output signals of the force controller in vector $\mathbf{U}$ are the desired values of the end-effector position, we speak about position based force control already mentioned. In [6] we investigated and compared simple approaches of position based force control using an industrial robot with its commercial robot controller. In this context the preferred algorithm was a simple proportional controller with positive feedback of the current robot position. In [7] and [8] this promising approach was used for the development of algorithms of two-dimensional force/position control and orientation control, which may be applied in some contour following tasks, e.g. in polishing, deburring or grinding.

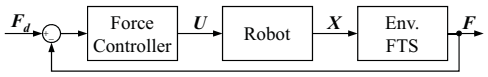

Fig. 1. General scheme of explicit force control.

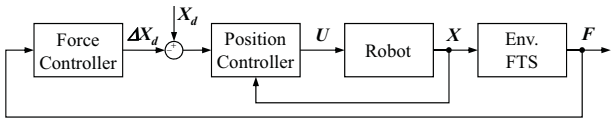

Fig. 2. General scheme of implicit force control.

In contrast to this, with implicit force control the desired values cannot be set directly. From the measured forces, the deviation vector $\mathbf{\Delta X_d}$ is calculated, which modifies the desired end-effector position given by vector $\mathbf{X_d}$ so that a defined contact force can arise. The basic structure of implicit force control shows the signal flow diagram of Fig. 2. We will here focus on the implicit force control of an industrial robot, but now and then we will bring implicit force control in relationship to explicit force control.

This paper is further organized as follows: In the next section some additional basics of robot force control will be shown. The experimental setup and the test procedure which will be used later to analyze different force control algorithms will be presented in section III. Thereafter, three general types of implicit force control namely stiffness control (section IV),

A. Winkler is with the Hochschule Mittweida, University of Applied Sciences, Mittweida, Germany (e-mail: alexander.winkler@hs-mittweida.de).
J. Suchý is with the University of Matej Bel, Banská Bystrica, Slovakia.

damping control (section V) and impedance control (section VI) will be investigated and verified on an industrial position controlled robot. Finally, in the last section a short conclusion is given.

II. Robot Force Control

As already mentioned, force control algorithms can be generally divided into explicit and implicit control. Another important fact when regarding force control algorithms is the type of actuating variable which is provided by the algorithm. In many publications it is assumed that there is access to the desired values of the joint torques of the robot. In this case the behavior of a robot can be described only by its dynamic equation:

$$\tau = \mathbf{M}(\mathbf{q})\ddot{\mathbf{q}} + \mathbf{C}(\mathbf{q}, \dot{\mathbf{q}})\dot{\mathbf{q}} + \mathbf{G}(\mathbf{q}) \tag{1}$$

In (1) τ is the vector of applied joint torques, vector $\mathbf{q}$ includes the joint angles, $\mathbf{M}$ is the inertia matrix, $\mathbf{C}$ represents the Coriolis and centrifugal forces/moments and $\mathbf{G}$ includes the gravitational forces/moments. If the values of $\mathbf{M}$, $\mathbf{C}$ and $\mathbf{G}$ are known, it may be possible to decouple and linearize the controlled plant, which will result in approaches denoted as model based control [9], [10], computed torque control [11], inverse dynamics control [12], etc.

However, industrial robots are usually position controlled in joint space using cascade control as a rule scheme and access to joint torques or motor currents is not enabled by the manufacturer. For that reason the dynamic model (1) is not practical for position controlled manipulators. Its characteristic is defined by structure and the parameters of the decentralized joint control. As already seen, using an industrial robot in force control mode, the force control loop has to be closed around the position control loop. The algorithms of implicit force control investigated in this paper are also position based approaches.

One general approach of implicit control is impedance control introduced by Hogan [13]. Mechanical impedance in the contact situation of robot and environment is given in one direction as follows:

$$\frac{F(s)}{[\Delta X_d(s)]\, s} = ms + d + \frac{c}{s} \tag{2}$$

where m, d and c are the parameters of mass, damping and stiffness. In contrast to this definition of the impedance often the relationship between force and position is used:

$$\frac{F(s)}{\Delta X_d(s)} = ms^2 + ds + c \tag{3}$$

For every Cartesian degree of freedom its mechanical impedance may be parameterized individually. The block diagram of position based impedance control can be seen in Fig. 3.

There are some special kinds of impedance control. One of it is stiffness control introduced by Salisbury [14]. He proposed an approach on the basis of the robot joint torques. For this purpose the Cartesian stiffness matrix $\mathbf{c}$ is transformed into joint space $\mathbf{c_q}$ using the Jacobian matrix $\mathbf{J}$ of the robot:

$$\mathbf{c_q} = \mathbf{J^T c\, J} \tag{4}$$

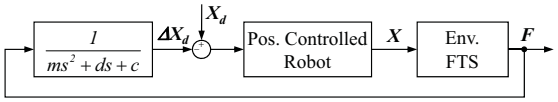

Fig. 3. Position based impedance control.

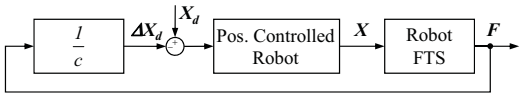

Fig. 4. Position based stiffness control.

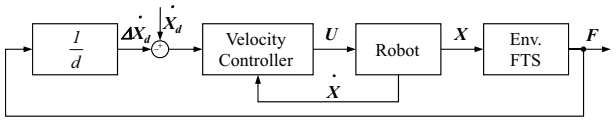

Fig. 5. Damping control.

Another type of stiffness control published e.g. in [1] and [15], uses Cartesian position correction values to control the robot manipulator instead of joint torques. Setting mass and damping in (3) to zero, the control law for one degree of freedom follows to:

$$\Delta X_d = \frac{1}{c} F \tag{5}$$

This leads to the signal flow diagram of the closed loop control which can be seen in Fig. 4. Assuming that the environment is located at position $X = 0$ and that it can be modeled just by its mechanical stiffness c_E the contact force in steady state will depend on the commanded position X_d:

$$F\,(t \to \infty) = \frac{c_E\, c}{c_E + c} X_d \tag{6}$$

One of the first published kind of impedance control is the damping control [16]. One possible signal flow diagram of damping control shows Fig. 5. As it can be seen, now the mass m and the stiffness c of the target impedance have been set to zero. According to the following control law the output signal of the damping controller is the desired velocity of the robot:

$$\Delta \dot{X}_d = \frac{1}{d} F \tag{7}$$

Hence, a contact force will result in a proportional change of the desired velocity. The contact force in steady state will reach the following value:

$$F(t \to \infty) = d\dot{X}_d \tag{8}$$

In the literature some modifications of damping control can be found, e.g. in [1] and [15] a combination of stiffness and damping control is proposed.

III. Experimental Setup

In the following sections primary types of implicit force control are investigated using the experimental equipment which can be seen in Fig. 6.

The manipulator is a six axes low payload robot of type KUKA KR6/2. It is controlled by the commercial robot

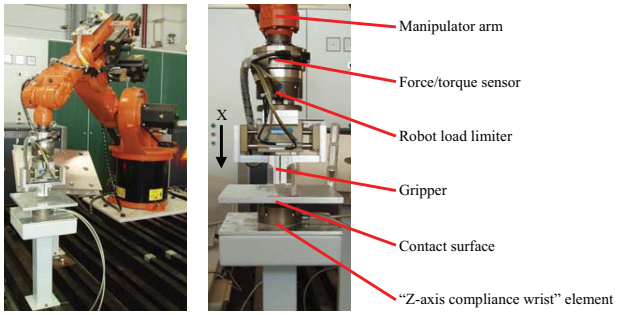

Fig. 6. Experimental setup used for experiments.

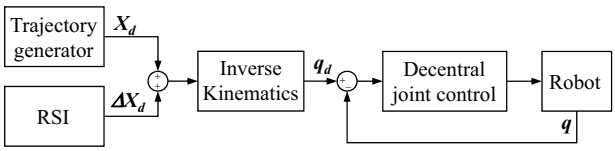

Fig. 7. Access to the position control loops using RSI.

controller KUKA KRC2. The robot is equipped with the six component force/torque sensor SCHUNK FT-Delta. From its measured values we use only the force component which is vertically orientated toward ground.

As in this paper position based force control approaches are investigated, it is necessary to have an access to the position control loops. This feature is available with the KUKA Robot Sensor Interface (RSI) [17], which allows the realization of sensor guided robot motions. Using RSI for the implementation of individual controllers, these algorithms will be executed in real time periodically within the interpolation cycle of $12\,ms$ in parallel to the user robot program written in KUKA Robot Language (KRL). It is possible to influence the end-effector position/orientation $\mathbf{X}$ by Cartesian position correction represented by vector $\mathbf{\Delta X_d}$ with respect to the desired position $\mathbf{X_d}$. The whole structure of motion control can be found in Fig 7, where $\mathbf{q_d}$ and $\mathbf{q}$ are the vectors of desired and current joint angles, respectively.

It is very difficult to find a model for the motion behavior of the RSI-controlled robot because we have not enough information about its internal control algorithms. One possibility to get it is experimental modeling, by recording step and frequency responses. An unfavorable fact is that the robot behavior includes some nonlinear parts, e.g. the difference between small-signal and large-signal behavior. The dynamics of the robot motion in one Cartesian DOF may be approximated be a first order system with time delay [18]. The transfer function $G_{Rob}(s)$ represents the relationship between commanded position X_d or position correction and the current end-effector position X:

$$G_{Rob}(s) = \frac{X(s)}{X_d(s)} = \frac{1}{1 + T_{Rob}s} e^{-sT_d}, \tag{9}$$

where T_{Rob} is assumed to be $0.5\,s$ and the time delay T_d is set to 3 interpolation cycles ($36\,ms$).

For the realization of a defined contact environment the so called "z-axis compliance wrist" element is used. The stiffness of the z-axis compliance wrist can be adjusted by the pressure of the compressed air. Assuming relatively low velocities of the robot during contacting the environment we can describe the environment by simple spring behavior

$$F = \left\{ \begin{array}{ll} c_E(X - X_E) & \text{for } X > X_E \\ 0 & \text{for } X \leq X_E \end{array} \right\}, \tag{10}$$

where c_E is the environment stiffness and X_E is the position of the contact surface in robot frame. The value of c_E in experiments presented here is $82\,N\,mm^{-1}$. It includes also the compliance of the robot caused by its mechanics, force/torque sensor, robot load limiter, etc.

Two different experiments are suitable to verify force control algorithms. First one is contact detection. Starting point of the robot end-effector is located in free space with a certain distance away from the environment surface. The task of the force controller is to establish the contact between end-effector and environment and reach a certain contact force. Criteria of the control quality are force overshoot and approaching velocity. In the second experiment we assume that the environment contact is already established. We modify the desired contact force value are recording step responses of the contact force. Here criteria of control quality are force overshoot and transient time.

IV. Stiffness Control

The signal flow diagram of stiffness control has been already shown in Fig. 4. With the help of the stiffness parameter c of the controller, the stiffness of the whole control system c_C consisting of position controlled robot and contact environment can be adjusted. Assuming that the position controlled robot has proportional behavior with transfer factor 1, with the help of the environment stiffness c_E, c_C can be determined as follows:

$$c_C = \frac{c_E c}{c_E + c} \tag{11}$$

So, hypothetically, the value of c_C can be modified between c_E and 0. However, decreasing c will bring the closed loop control closer to the stability margin.

Using the transfer function of the position controlled robot $G_{Rob}(s)$, introduced already in section III and taking only the stiffness parameter of the mechanical impedance of the environment into consideration, the transfer function of the closed loop control $G_C(s)$ can be written as follows (see also Fig. 4):

$$G_C(s) = \frac{F(s)}{X_d(s)} = \frac{G_{Rob}(s)c_E}{1 + G_{Rob}(s)c_E c^{-1}} \tag{12}$$

The static transfer factor of $G_C(s)$ represents the relationship between force and position change.

There are different possibilities for the implementation of the simple concept of position based stiffness control, depending on the practical robot controller. Very important is the fact, how the robot responds to a rapid change of the desired position X_d or ΔX_d, especially when the end-effector is located relatively far from the environment. It may be suitable to integrate additional low pass filter into the controller

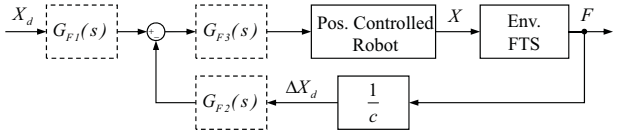

Fig. 8. Position based stiffness control with low pass filters.

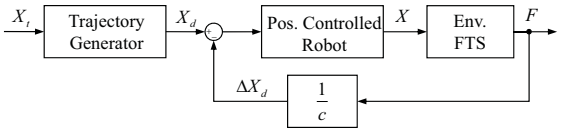

Fig. 9. Position based stiffness control with trajectory generator.

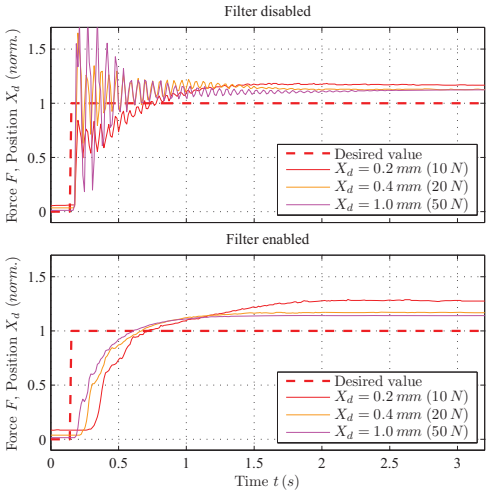

Fig. 10. Experimental results of position based stiffness control.

structure to prevent abrupt signal changes. Thereto, Fig. 8 shows some possibilities where the filter can be included. Keeping the fundamental behavior of stiffness control filter $G_{F1}(s)$ should be preferred because in that case only signal X_d will be smoothed. Using filter $G_{F2}(s)$ or $G_{F3}(s)$ in principle the signal of the contract force will be additionally filtered, which leads to a time delay in the closed control loop.

As can be seen in Fig. 9, it may be also possible to use the trajectory generator of the robot controller to avoid rapid end-effector motions. Based on the target position X_t the trajectory generator computes the time series of the desired position X_d, e.g. using linear continuous path interpolation.

The functioning of stiffness control in the experiment is shown in Fig. 10. For this purpose two different types are implemented into the robot controller. First one is position based stiffness control as in Fig. 4. Second one uses additional low pass filter $G_{F1}(s)$ for smoothing X_d, see also Fig. 8. In both cases the target stiffness c_C is chosen to be $50\,N\,mm^{-1}$. With the value of the environment stiffness $c_E = 82\,N\,mm^{-1}$ the controller gain c can be calculated as follows to $128\,N\,mm^{-1}$:

$$c = \frac{c_E c_C}{c_E - c_C} \tag{13}$$

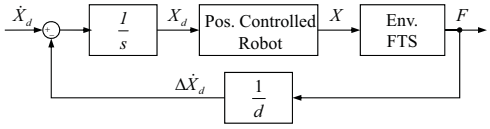

Fig. 11. Position based damping control.

In the experiment the robot end-effector is already in contact with the environment. We have precalculated three position values of $0.2\,mm$, $0.4\,mm$ and $1.0\,mm$ which represent a contact force of $10\,N$, $20\,N$ and $50\,N$, respectively. The desired end-effector position was changed rapidly. Regarding Fig. 10 it can be seen, that in the case when the filter $G_{F1}(p)$ is disabled, the step response of the contact force strongly oscillates, which makes this version of stiffness control useless, especially when higher values of the contact force should be reached. Stiffness control may be improved by activating the low pass filter in the branch of the desired position. Corresponding step responses can also be seen in Fig. 10. For this purpose first order low pass filter was used:

$$G_{F1}(s) = \frac{1}{1 + T_F s} \tag{14}$$

Its time constant T_F was chosen to $0.2\,s$.

Using a position controlled robot, stiffness control can be related to proportional controller of explicit controller domain. In the case that we do not know the position of the environment and the robot end-effector is located in free space, stiffness control will not work successfully.

V. Damping Control

Another type of implicit force control is damping control. One version can be seen in Fig. 5. However, access to the velocity controller is often not available with an industrial robot. Having access to the desired position in Cartesian space, one possible realization of damping control is shown in Fig. 11.

As it can be demonstrated in contrast to stiffness control, now the static value of the contact force is independent from the environment stiffness. According to (8) the contact force in steady state depends only on the damping parameter of the controller d and on the value of the desired velocity $\dot{X}_d$. From the signal flow diagram of Fig. 11 the transfer function of the closed loop control can be determined:

$$G_C(s) = \frac{F(s)}{X_d(s)s} = \frac{G_{Rob}(s)c_E}{G_{Rob}(s)c_E d^{-1} + s} \tag{15}$$

Comparing damping control with position based approaches to explicit force control, it may be related to integral control. Regarding the integral force controller acting on a position controlled robot [6], it can be recognized that the velocity of the robot motion is proportional with respect to the force control error. Using damping control the contact force is proportional with respect to the desired velocity. So the advantage in comparison to stiffness control is that damping control is also practical to establish the contact between robot and environment approaching the environment from free space.

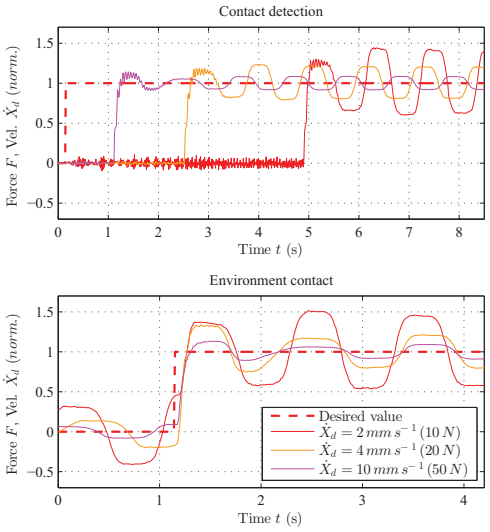

Fig. 12. Experimental Results of damping control.

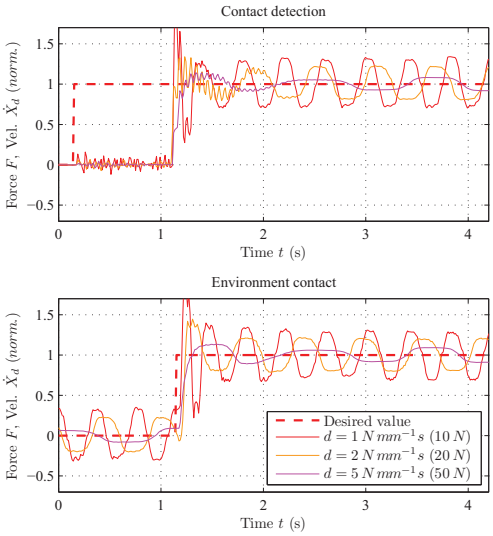

Fig. 13. Experimental results of damping control when modifying the damping parameter.

The dilemma of the integral controller [6] can be also assigned to damping control. On the one hand when the robot end-effector is located in free space the goal is to reach a relatively high approach velocity of the robot to contact the environment. So the controller gain should be chosen as high as possible, which means that damping parameter should be as low as possible. On the other hand, when the robot is in contact with the environment the closed control loop has to be stable and oscillations of the force should be prevented. Due to this it seems to be convenient to switch the controller gains in dependence on the contact situation [6].

In the experiments presented in this paper controller gain d of damping control will be optimized to fast contact establishment. In the first experiment the following setting will be selected: In the case that the desired value of the contact force is $50\,N$, the robot should move toward the contact surface with desired velocity of $\dot{X}_d = 10\,mm\,s^{-1}$. So, according to (8) damping parameter d has been chosen $5\,N\,mm^{-1}s$. Fig. 12 shows the contact forces both in the scenario of contacting the environment from free space and in the scenario when the environment contact is already established. In both cases different values of $\dot{X}$ are used to reach different values of the contact force. First, it can be seen that the smaller the velocity the longer the time before getting environmental contact. After the contact is established an oscillation of the force value can recognized. This oscillation may be arisen by the resolution of the robot position. The amplitude of the force oscillations can be reduced by increasing damping d. However, the desired velocity $\dot{X}_d$ has to be decreased to hold the force value.

Modifying the damping d is the second possibility to adjust the contact force. For this purpose the value of $\dot{X}_d$ will be kept constant. In our experiment $\dot{X}_d$ is set to $10\,mm\,s^{-1}$. Caused by the relative fast approach velocity the force overshoot is high, especially when the desired force is low, see Fig. 13. The permanent force oscillation can be recognized again when the robot is in contact with the environment.

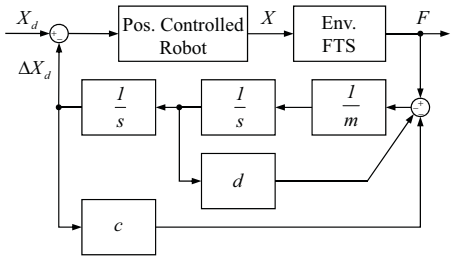

Fig. 14. Impedance control.

VI. Impedance Control

Impedance control, which takes the full mechanical impedance into consideration, is the general type of implicit force control. The concept of position based impedance control was already introduced in Fig. 3. Fig. 14 shows the signal flow diagram of impedance control for one degree of freedom. As can be seen, the impedance term was decomposed. The corresponding closed loop transfer function follows to:

$$G_C(s) = \frac{F(s)}{X_d(s)} = \frac{G_{Rob}(s)c_E\left(c + d\,s + m\,s^2\right)}{G_{Rob}(s)c_E + c + d\,s + m\,s^2} \qquad (16)$$

With virtual mass m, in comparison to stiffness control or damping control, additional inertia will be integrated into the system. It may be reasoned that when contacting the environment stability problems occur, especially in the case if the contact surface is stiff.

However, impedance control plays an important role in the force based human-robot interaction [19]. It is possible to define the target impedance for every Cartesian degree of freedom or in joint space for every joint within a certain range individually. Setting stiffness parameter $c = 0$ will result in mass-damper system which can be applied to the so called

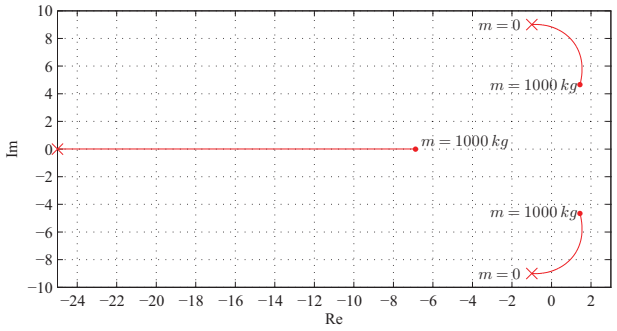

Fig. 15. Root locus of the mass-damper system with respect to mass as parameter.

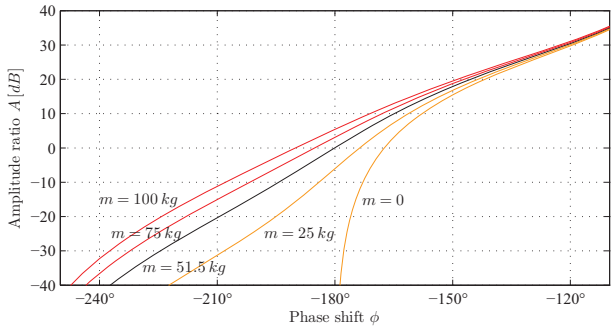

Fig. 16. Nichols chart of the mass-damper system with different values of the mass parameter.

hand guidance. Here the human operator takes the robot arm and moves it through the workspace. Hand guidance of robot manipulators may be used for intuitive robot programming or to human robot cooperation. In the case that stiffness is activated, i.e. $c > 0$, the manipulator has the behavior of a spring-mass-damper system. Then, during hand guidance robot would move back to the start position when interaction forces disappeared.

The destabilizing property of impedance control described in [20] will be now demonstrated on a short example. For this purpose we take the damping controller from the previous section with $d = 2N\,mm^{-1}s$ and add a variable mass. The impedance controller has then the behavior of a mass-damper system. The closed loop transfer function can be reduced to:

$$G_C(s) = \frac{F(s)}{X_d(s)} = \frac{G_{Rob}(s)c_E\left(d\,s + m\,s^2\right)}{G_{Rob}(s)c_E + d\,s + m\,s^2} \qquad (17)$$

Taking (9) and neglecting the dead time, the behavior of the position controlled robot can be simplified to first order system

$$G_{Rob}(s) = \frac{1}{1 + T_{Rob}s}, \qquad (18)$$

where the time constant T_{Rob} has a value of $0.5\,s$. The closed loop transfer function results in:

$$G_C(s) = \frac{d\,s + m\,s^2}{1 + \frac{d}{c_E}s + \frac{T_{Rob}d+m}{c_E}s^2 + \frac{T_{Rob}m}{c_E}s^3} \qquad (19)$$

Fig. 15 shows the root locus of the closed control loop with respect to the mass m of the target impedance. Its value has been modified between 0 and $1000\,kg$. The stability margin can be found where the root locus reaches the right s-half-plane. In the example presented here, the critical mass is approximately $51.5\,kg$. One may come to the same conclusion for Nichols chart (Fig. 16). It is based on the transfer function of the open control loop:

$$G_O(s) = \frac{c_E}{d\,s + (T_{Rob}d + m)\,s^2 + T_{Rob}m\,s^3} \qquad (20)$$

The Nichols chart shows the amplitude ratio as a function of the phase shift. The chart can be subdivided by $0\,dB$-axis and by $-180°$-axis into quadrants. When the graph passes the second quadrant (top left) the closed control loop will be unstable. The already shown stability margin, can be found again.

VII. Conclusion

In this paper some basic algorithms of implicit robot force control, namely stiffness control, damping control and impedance control, were selected for the implementation with an industrial robot. For this purpose the corresponding approaches have been adapted to position based controller structures, which are realizable with a position controlled robot. To parameterize robot controller some relationships between commanded robot motion/position, parameters of the contact environment and controller parameters are worked out. This may be necessary to calculate the static value of the contact force.

As for the stiffness controller it can be recognized that its behavior is similar to the behavior of the proportional controller of explicit force control. This means that it can be only used in the case when the contact between robot and environment is already established. When the robot is located in free space and the distance between its end-effector and the contact surface is unknown, stiffness controller is not suitable.

Damping controller is similar to integral controller. Therefore, it can be used in both situations, i.e. contacting the environment from free space or when the robot is already in contact with the environment. It can be learned from integral controller [6], that optimal controller gain (damping) for contact detection is different from optimal gain/damping in contact situation.

Finally, impedance control with structure of full mechanical impedance is not suitable when the robot is in contact with the environment, because the mass component can be seen as a source of instability. An example was worked out to demonstrate this fact by simulation. However, impedance control may be used for some kinds of human-robot interaction.

References

[1] G. Zeng and A. Hemami, "An overview of robot force control," *Robotica*, vol. 15, no. 5, pp. 473–482, 1997.
[2] M. Vukobratović and A. Tuneski, "Contact control concepts in manipulation robotics–an overview," *IEEE Transactions on Industrial Electronics*, vol. 41, no. 1, pp. 12–24, 1994.
[3] R. Volpe and P. Khosla, "A theoretical and experimental investigation of explicit force control strategies for manipulators," *IEEE Transactions on Automatic Control*, vol. 38, no. 11, pp. 1634–1650, 1993.

[4] J. De Schutter and H. Van Brussels, "Compliant robot motion I. A formalism for specifying compliant motion tasks," *International Journal of Robotics Research*, vol. 7, no. 4, pp. 3–17, 1988.
[5] E. Dégoulange and P. Dauchez, "External force control of an industrial PUMA 560 robot," *Journal of Robotic Systems*, vol. 11, no. 6, pp. 523–540, 1994.
[6] A. Winkler and J. Suchý, "Position feedback in force control of industrial manipulators – an experimental comparison with basic algorithms," in *IEEE International Symposium on Robotic and Sensors Environments*, 2012, pp. 31–36.
[7] ——, "Force controlled contour following on unknown objects with an industrial robot," in *IEEE International Symposium on Robotic and Sensors Environments*, 2013, pp. 208–213.
[8] ——, "Force controlled contour following by an industrial robot on unknown objects with tool orientation control," in *Proc. of Joint Conference on Robotics – 45th International Symposium on Robotics and 8th German Conference on Robotics*, 2014.
[9] J. J. Craig, *Introduction to Robotics Mechanics and Control*. Pearson Prentice Hall, 2005.
[10] T. A. Lasky and T. C. Hsia, "Force control of robotic manipulators," in *Applied Control*, S. G. S. G. Tzafesta, Ed. Marcel Decker, 1993, ch. 22, pp. 639–661.
[11] A. A. Goldenberg, "Implementation of force and impedance control in robot manipulators," in *Proc. of IEEE International Conference on Robotics and Automation*, vol. 3, 1988, pp. 1626–1632.
[12] C. Natale, B. Siciliano, and L. Villani, "Robust hybrid force/position control with experiments on an industrial robot," in *Proc. of the IEEE/ASME International Conference on Advanced Intelligent Mechatronics*, 1999, pp. 956–960.
[13] N. Hogan, "Impedance control, an approach to manipulation: Part i, ii, iii," *ASME Journal of Dynamic Systems, Measurement and Control*, vol. 107, pp. 1–24, 1985.
[14] J. K. Salisbury, "Active stiffness control of a manipulator in cartesian coordinates," in *Proceedings of the IEEE International Conference on Decision and Control*, vol. 19, 1980, pp. 95–100.
[15] D. E. Whitney, "Historical perspective and state of the art in robot force control," *International Journal of Robotics Research*, vol. 6, no. 1, pp. 3–14, 1987.
[16] ——, "Force feedback control of manipulator fine motions," *Journal of Dynamic Systems, Measurement and Control*, vol. 99, no. 2, pp. 91–97, 1977.
[17] KUKA Roboter GmbH, *KUKA.RobotSensorInterface (RSI) 2.1*, 2007.
[18] A. Winkler and J. Suchý, "An approach to compliant motion of an industrial manipulator," in *Proc. of the 8th International IFAC Symposium on Robot Control*, 2006.
[19] ——, "Possibilities of force based interaction with robot manipulators," in *Human-Robot-Interaction*, N. Sarkar, Ed. I-Tech Education and Publishing, 2007, pp. 445–468.
[20] N. Hogan and S. P. Buerger, "Impedance and interaction control," in *Robotics and Automation Handbook*, T. R. Kurfess, Ed. CRC Press, 2004, ch. 19.